

Modelle für Wetter & Umwelt

# COSMO-CLM: Influence of Grid Resolution on Precipitation Forecast

Robert Wright

24<sup>th</sup> July 2023

## 1. Introduction

In 1952, the *Met Office*, i.e., the UK's national weather service, successfully completed its first numerical weather prediction forecast on a  $12 \times 8$  grid with grid point spacing of 260 km [1]. Since then, weather forecasts have improved tremendously, not least because of an increase in grid resolution. This development has been made possible by the continued growth of available computational power. While, on the one hand, increased grid resolution undoubtedly improved the numerical weather forecast, on the other hand, it also increased the need for adequate computational resources. The CFL criterion introduces an upper limit for the time step proportional to the grid point separation—a high grid resolution thus demands a short time step, which is computationally more expensive. Therefore, it is of interest to understand the influence of grid resolution on numerical weather prediction in order to find the best compromise of grid point spacing in terms of computing

time and forecast quality. In this study, a regional weather model calculates one-month forecasts on three different spatial resolutions for the region of Europe. Then, the change in precipitation patterns due to varying grid size is analysed. Generally speaking, precipitation plays a major role in weather forecasts, hence, it seems natural to use this variable in order to compare grid resolution. On top, as a diagnostic variable, it is based on multiple direct model predictions and captures the effects of resolution-dependent internal model dynamics.

## 2. Model setup & data

The COSMO model in CLimate Mode (CCLM) is the climate version of the COSMO model, that has been designed for operational mesoscale numerical weather prediction. CCLM, as a limited-area atmospheric model, receives boundary and initial conditions from a driving host model, or, in our case study, from ERA-Interim reanalysis data (resolution of  $0.75^\circ$ ). Time integration relies on a third-order Runge-Kutta scheme. The number of both vertical and soil levels is equal to 10. The model equations are formulated in rotated geographical coordinates to reduce the effect of varying grid cell size. Parametrization for grid-scale clouds and precipitation is based on a Kessler-type bulk formulation, which uses specific grouping of particles into broad categories of water substance (e.g., cloud water) that interact by various microphysical processes. The implemented cloud ice scheme allows explicit representation of ice clouds. While vertical turbulent diffusion parametrization is based on a prognostic equation for turbulent kinetic energy, as far as I am concerned, no subgrid-scale (deep) convection scheme is included by default<sup>1</sup>. The time step has been set to 150 s for all grid resolutions. For further information about the COSMO model please refer to Schättler et al. [2].

The study is composed of three CCLM simulations during January 1990, as introduced in table 1. This period of time has been chosen as grid definition files and appropriately scaled boundary conditions were already available. Figure 1 displays the mean precipitation within the entire model domain, however, structures of ‘unphysical’ values are

---

<sup>1</sup> `itype_conv` undefined in model namelists

Experiment name	Resolution [°]	Grid	Spacing [ $\approx$ km]
02°	0.2	$280 \times 230$	25
05°	0.5	$100 \times 80$	65
1°	1	$56 \times 46$	130

Table 1: CCLM simulations of this study

clearly visible at the edges, where interpolation between model predictions and constraining boundary conditions distorts the results. In the following, the region of interest is reduced to the area within the red rectangle in fig. 1. It is notable that the 05°-simulation region seems to be cropped in the north and east compared to the other simulations. This is due to an erroneous value in the number of grid points during grid definition, but will not affect the results as the region of analysis is still sufficiently large.

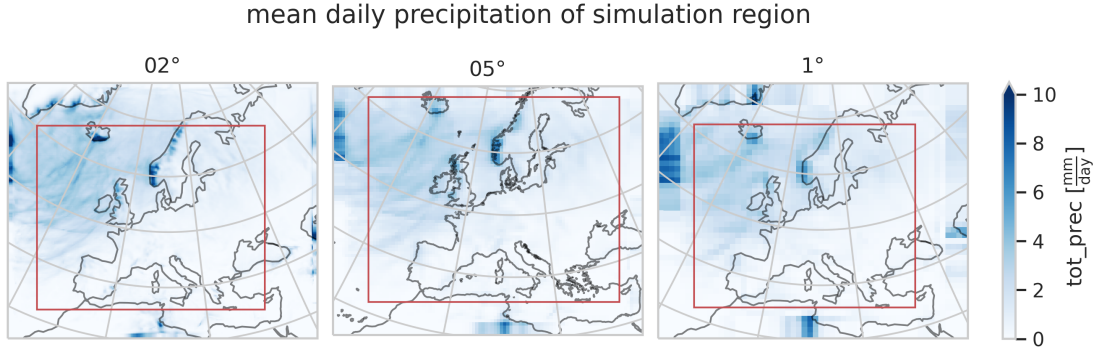


Figure 1: Spatial domains of simulations. Red rectangle indicates area of analysis. Please note that here and in the following figures pointed ends of a colourbar indicate existing out-of-range values.

In this study, ERA5 reanalysis data produced by the ECMWF serves as a reference. Although also a model product themselves, reanalyses assimilate observational records and thus are a reasonable choice to compare simulation output against. ERA5 data is provided on a  $0.28^\circ$  grid, however, the data is remapped to a  $0.2^\circ$  rotated grid to be able to cut the same region as in the CCLM simulations (see fig. 1).

The shell script for data processing, python code for re-creating all figures as well as further comments can be found in the corresponding online repository<sup>2</sup>. Much data processing has

<sup>2</sup><https://gitlab.met.fu-berlin.de/rw0064fu/mwu-gridres>

been realized by using *Climate Data Operators* of Schulzweida [3].

### 3. Results & Discussion

Figure 2 illustrates the spatial distribution of mean precipitation: The general pattern of different grid resolutions is similar, depicting high precipitation rates over the Northern Atlantic and at the coasts of Iceland, Norway and Scotland. However, it is evident that using high grid resolution locally increases the intensity of precipitation.

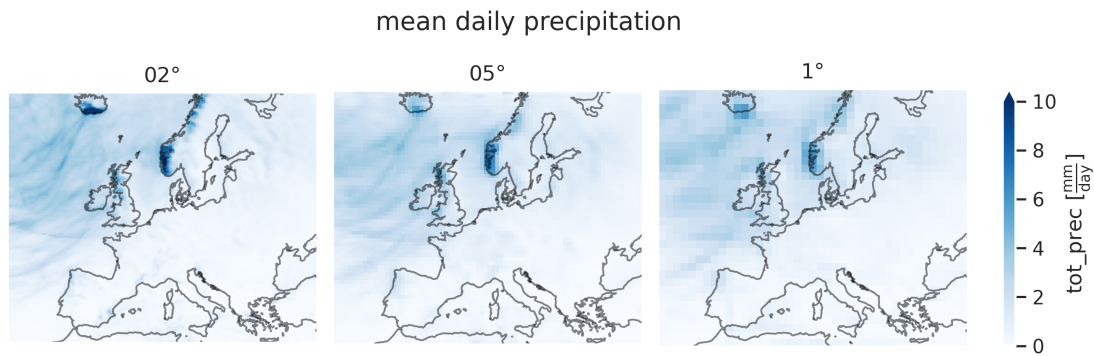


Figure 2: Temporal mean of daily precipitation sum throughout January 1990 for different grid resolutions.

When focussing on the temporal domain, the daily precipitation signals of the CCLM simulations are—generally speaking—similar, indicating that the daily sum over the entire (cropped) model region does not change considerably with model resolution. In fig. 3, precipitation is split into a grid-scale and convective component, and ERA5 data is included as a reference. In both subplots, simulations underestimate the observed daily precipitation sum, although the difference between reference and simulation is more pronounced for convective precipitation. The underlying trend in simulation and reference of grid-scale precipitation is comparable, which validates the model results on broader scales. It is important to note though that the simulations have been driven with ERA-Interim data and are now compared to ERA5 data, which might introduce additional biases triggered by different data assimilation procedures of the reanalyses.

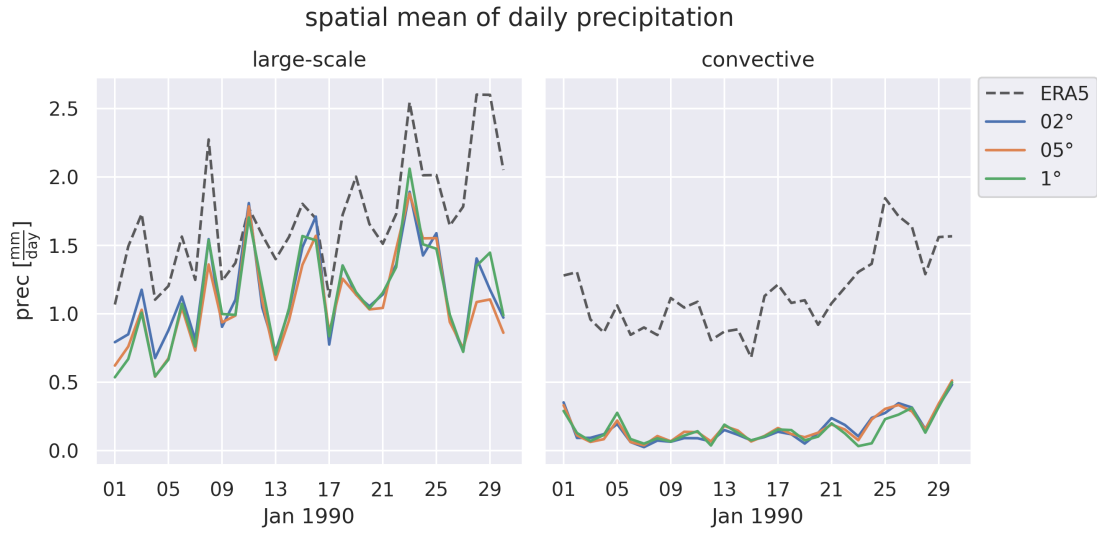


Figure 3: Spatial mean of daily precipitation sum split into large-scale (i.e., grid-scale) and convective signal for different grid resolutions. ERA5 reanalysis data as reference.

The *absolute* difference in precipitation between grid resolutions is more pronounced in the grid-scale precipitation, although without a consistent signal. E.g., in the beginning of January,  $0.2^\circ$ -resolution shows more grid-scale precipitation compared to the remaining resolutions, in the end of the month though,  $0.2^\circ$ - and  $1^\circ$ -resolution show a similar signal, while  $0.5^\circ$ -resolution simulates less grid-scale precipitation. In contrast, variation in the convective part is relatively small. The missing deep convection scheme might be the reason for this observation, since in such a case convective precipitation is derived from vertical turbulence only.

One way to combine information from the spatial and temporal domain is displayed in fig. 4. The Hovmöller diagram illustrates how precipitation events follow the dominant westerly flow of the Northern Hemisphere. On top, precipitation is more intense in the western part of the model region (as already indicated by fig. 2, especially over the Atlantic Ocean), and starts to decrease over the land masses of Northern and Central Europe. Again, simulated precipitation underestimates the reanalysis data in the entire model region. In particular, the presumably convective events at  $-5^\circ$  to  $0^\circ$  rotated longitude are not present in the simulations (apart from one in mid-January). The high grid resolution has a strong localization of precipitation extremes, but tends to underestimate their

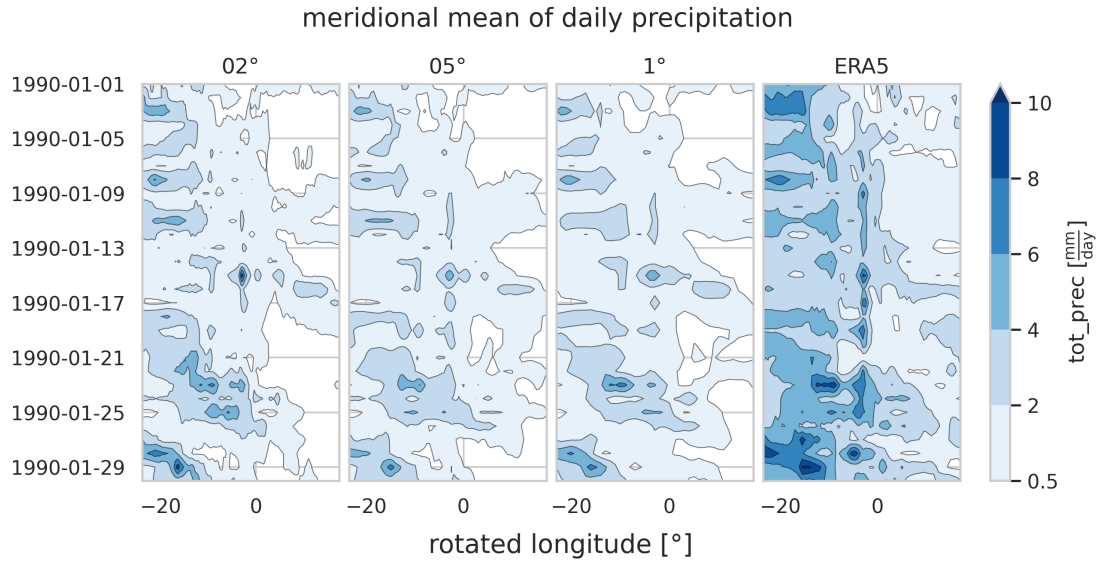


Figure 4: Hovmöller plot of the meridional mean of daily precipitation sum on the  $x$ -axis (units in *rotated* longitude) and time domain in days on  $y$ -axis. CCLM simulations of different grid resolution and ERA5 reanalysis data displayed. Precipitation below  $0.5 \text{ mm d}^{-1}$  is excluded.

spread. For example, in the end of January, the  $0.2^\circ$ -resolution shows small-scale structures of intense precipitation in the west, but fails to simulate the large area of moderate precipitation further in the east. The lower resolutions cannot reproduce the intensity of the strong events in the west, but the  $1^\circ$ -resolution shows zonal precipitation structures until far into the east, which match the pattern of the reanalysis data. For further details about this individual event refer to fig. 5 in appendix A.

## 4. Conclusion

This study provides details about the influence of different grid resolutions on precipitation forecasts using the CCLM regional climate model. High grid resolution (expectedly) improves localization of the precipitation events. Differences in precipitation intensity are clearly visible on maps, but almost disappear when averaging over a sufficiently large region. Precise localization of precipitation events implies higher number of grid boxes

without precipitation, which results in similar precipitation signals when averaging, regardless of the grid resolution. The remaining differences in precipitation for changing grid sizes are mainly found in grid-scale precipitation, although this might change if a deep convection scheme is enabled in the model runs. To summarize, if precise forecasts of intensity and location are of interest, it is vital to increase the grid resolution, however, low grid resolutions can already capture precipitation structures and become increasingly useful, if data availability allows averaging or other applications of simple statistics. These qualitative results could be extended by running ensemble forecasts with perturbed initial and boundary conditions to get an idea of the underlying uncertainty. Additionally, the expected increase in the ratio of convective to grid-scale precipitation in the summer months (JJA) could complement the results if analysis is repeated for such different atmospheric conditions.

## References

- [1] Meteorological Office. *History of numerical weather prediction*. 2023. URL: <https://www.metoffice.gov.uk/weather/learn-about/how-forecasts-are-made/computer-models/history-of-numerical-weather-prediction> (visited on 24/07/2023).
- [2] U. Schättler et al. *COSMO-Model Version 6.00: A Description of the Nonhydrostatic Regional COSMO-Model - Part VII: User's Guide*. COSMO Consortium for Small-Scale Modelling, 2021. DOI: 10.5676/DWD\_PUB/NWV/COSMO-DOC\_6.00\_VII.
- [3] U. Schulzweida. *CDO User Guide*. Version 2.1.0. Oct. 2022. DOI: 10.5281/zenodo.7112925.



## A. Supplementary material

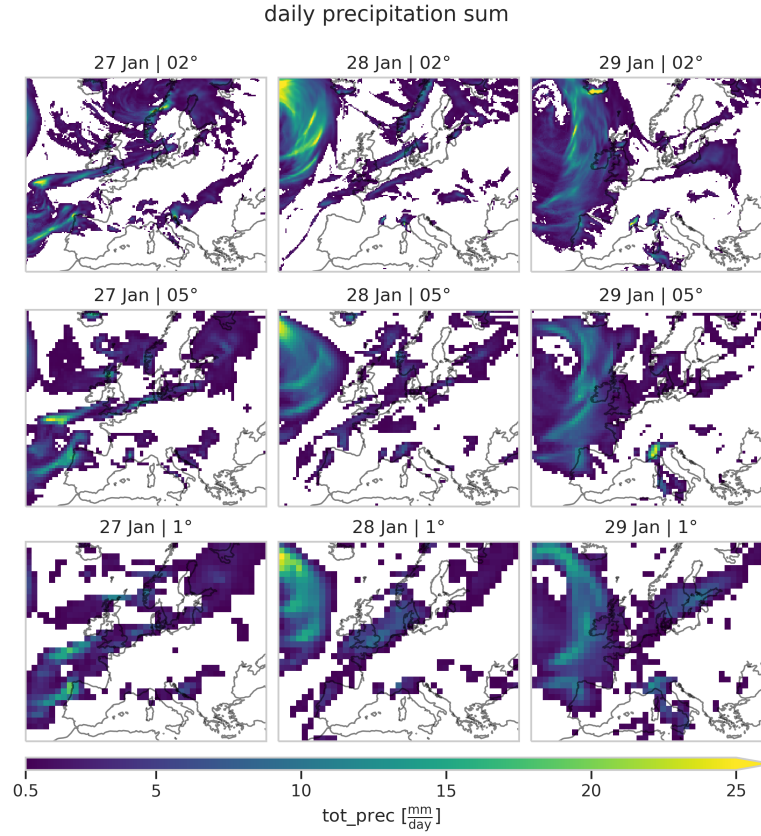


Figure 5: Maps of daily precipitation sum during event from 27 to 29 Jan (shortly after [Cyclone Daria](#)). Identical grid resolutions are displayed row-wise, while columns represent single days. Precipitation below  $0.5 \text{ mm d}^{-1}$  is excluded. When focusing on the differences among grid resolutions, it is notable that (a)  $1^\circ$ -resolution displays large areas of precipitation in Northeastern Europe, while (b)  $0.2^\circ$ -resolution rather shows high intensities over the Atlantic Ocean and Iceland. Interestingly, solely  $0.5^\circ$ -resolution captures *strong* precipitation event over southwestern Alps on 29 Jan, which indicates the complexity of assessing effects of changing grid resolution.